PHYSICAL REVIEW B **73**, 184114 (2006)

Structural and electronic transitions in potassium-doped pentacene

Anders Hansson,* Johan Böhlin,† and Sven Stafström‡
Department of Physics and Measurement Technology, IFM, Linköping University, S-581 83 Linköping, Sweden

(Received 11 October 2005; published 17 May 2006)

We calculate the ground state geometrical structure of potassium-intercalated pentacene lattices using molecular mechanics and the density-functional theory. Both methods result in a structural phase transition in going from the pristine form to the intercalated state with one potassium ion per pentacene molecule. The phase transition is characterized by a sliding of adjacent pentacene molecules relative to each other. The electronic properties of this phase is studied with the density-functional theory. As a result of the geometrical changes, the π-π overlap in the direction perpendicular to the molecular planes of the layered pristine pentacene structure increases substantially and many of the electronic bands show strong dispersion in this direction. The Fermi energy of the doped phase appears in the middle of the conduction band where the density of states is maximum. The bandwidth of the conduction band is 0.7 eV.

DOI: 10.1103/PhysRevB.73.184114 PACS number(s): 61.66.Hq, 71.15.Mb, 71.20.Rv

I. INTRODUCTION

Organic semiconductors have, during the past 20 years, attracted a broad interest due to their possible applications in electronic and optoelectronic devices.[1–3] Pentacene ($C_{22}H_{14}$, abbreviated PEN here after), in particular, has been widely studied as a molecular conductor with very high charge carrier mobility and highly anisotropic charge transport.[4,5] Mobilities of $1\ \mathrm{cm}^2/\mathrm{V\,s}$ were reported at 300 K, and even higher values have been obtained more recently.[6] Such high mobilities, which are comparable or even better than in amorphous silicon at room temperature,[7] can only be obtained in systems with a high structural order and with particular intermolecular arrangements. Thus, the relationship between geometrical structure and electronic properties of molecular crystals is very important, and changes in the geometry will inevitably lead to changes in the electronic structure. In its pristine form PEN crystallizes in a layered structure with a herringbone arrangement of the molecules within the layers. Depending on preparation conditions and techniques, several different PEN crystal structures can be obtained.[8] Theoretical studies of the relation between the crystal structure and the electronic properties have, however, only been performed on the most stable of these polymorphs.[9,10]

An interesting feature of PEN is the conductivity enhancement achieved by doping.[11–14] Similar to other doped carbon based materials such as conjugated polymers and carbon nanotubes, stable amphoteric doping can also be achieved in PEN. From the device point of view, the interest in doping is not only a question of conductivity but is also related to the fact that the presence of dopants can improve charge injection properties of molecular electronic devices.[15] A structural analysis of iodine-doped PEN shows that there is a phase of intermediate iodine concentration for which the iodine ions intercalate between the PEN layers and also a phase, at higher doping concentrations, in which the iodine ions are located between PEN molecules in the plane.[16] In the case of donor doping, alkali metals such as Li (Ref. 14) as well as Na, K, and Rb (Ref. 12) have been studied. No structural analysis has, however, been reported for these phases. Measurements of the magnetic properties of potassium-doped PEN show an interesting low temperature hysteresis indicating a magnetic and possibly also a structural transition taking place in this material.[17] Thus, there are strong experimental evidences for structural transitions to occur as a function of doping concentration, both for iodine and potassium doping, and it is of large interest to get a deeper understanding of the relation between the stability of various structural phases and doping concentration.

In this work we present results from structural optimization calculations on potassium-doped molecular crystals. The results are obtained from molecular dynamics (MD) and density-functional theory (DFT) studies of PEN intercalated with potassium. We focus our studies on the structural phase transitions as a function of potassium concentration. In particular, we identify a more stable phase for the doped PEN crystal, where the herringbone structure is replaced by a π-stack arrangement. The electronic band structure and the density of states of this phase are also calculated and discussed in relation to the structural properties. For comparison, we also study a metastable layered phase of the same compound and discuss the differences in anisotropy in the electronic properties between these two phases.

II. METHODOLOGY

We carried out MD to equilibrate the system and quenched the structures by minimizing the energy, thus finding the optimum stoichiometry for the different doped systems.[18] We assumed that all potassium ions are fully ionized to K^+ and that the charges on PEN were distributed uniformly over the hole molecule. The force field used was chemistry at Harvard molecular mechanics (CHARMM).[19–21]

DFT calculations were then performed on both ground state and metastable structures obtained from the MD calculations. The DFT calculations were performed with the Vienna *ab initio* simulation package (VASP).[22–24] As an exchange correlation functional we used the generalized gradient approximation (GGA) *PW*91.[25,26] The super cells of the crystals were treated with periodic boundary conditions. In the basis set of the employed Blöchl's projector augmented wave (PAW) method, all plane waves with a kinetic energy lower than 400 eV were included. The projections were done in real space. According to the Monkhorst-Pack scheme, the Brillouin zone (BZ) was sampled with a Γ-centered mesh with $5\times5\times5$ points. The electronic minimization was performed with the preconditioned residual minimization method-direct inversion in the iterative subspace (RMM-DIIS) algorithm. Ions, shape, and volume of the super cell were relaxed with a conjugated gradient algorithm followed by the RMM-DIIS algorithm. The tolerances for the electronic and ionic relaxation were 10 μeV and 50 meV/Å, respectively.

It should be noted that the CHARMM force field includes an "exponential-6" potential which describes the nonbonded interactions. This potential accounts for both dispersive forces and interactions due to an intermolecular overlap of the charge density. In the GGA calculations, the dispersive interactions are to some extent missing. However, from the results presented below we observe a fairly strong intermolecular overlap and also very good agreement between our calculated lattice parameter for pristine pentacene and those obtained from crystallography data. This justifies the use of GGA for this type of molecular systems.

III. RESULTS AND DISCUSSION

In all calculations the super cell contains two PEN molecules, and in addition a varying number of potassium ions. The first system we consider is with one potassium ion per super cell, $K_1(C_{22}H_{14})_2$. A geometrical comparison between the ground states of the pristine and the $K_1(C_{22}H_{14})_2$ systems shows a similar result to that of Ito *et al.*,[16] the PEN molecules become almost parallel to the **c** direction (perpendicular to the PEN layer) when the dopant is added, which is similar to the structure of PEN thin films.[16] The herringbone arrangement of the PEN molecules is, however, unchanged. Potassium intercalates between the PEN molecular layers but there is no notable extension of the system in the direction perpendicular to the molecular plane, which shows that the potassium ions occupy empty positions in the plane separating two PEN layers.

However, when the potassium concentration is increased to $K_2(C_{22}H_{14})_2$, the equilibrium structure changes dramatically. The PEN molecules translate relative to each other breaking the layered structure of the pristine and lightly doped phases. In the new phase (*a* phase), shown at the top in Fig. 1, one of the two PEN molecules in the super cell is shifted by half a lattice vector both in the **a** and **c** directions. The triclinic Braivais lattice parameters are $a=6.8084$ Å, $b=7.7791$ Å, $c=14.6795$ Å, $\alpha=82.191°$, $\beta=84.216°$, and $\gamma=94.871°$. Furthermore, the herringbone arrangement, which is present in pristine and lightly doped samples has disappeared and the normal to the molecular plane now points in the same direction for both molecules in the super cell. This results in a π-stack arrangement for which neighboring PEN molecules overlap by approximately 1.5 hexagons or eight carbon atoms. The shortest contact distance within the π stack is C-C 3.25 Å, which is slightly smaller than in graphite and allows for a substantial intermolecular interaction as will be seen from the electronic band structure diagrams below.

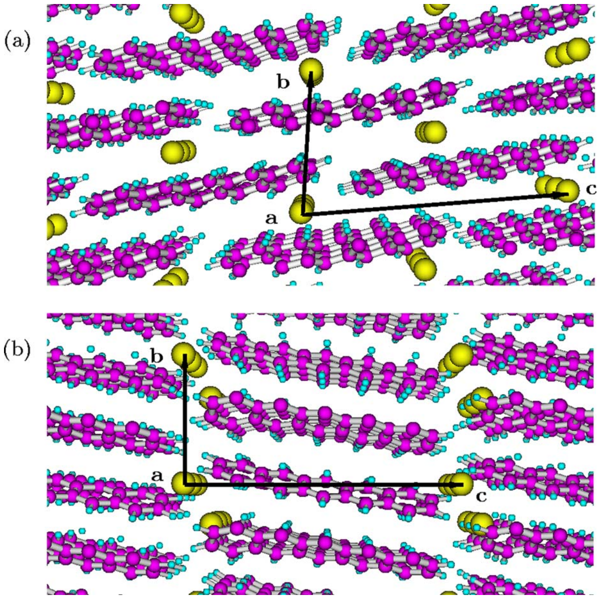

FIG. 1. (Color online) Crystal structure of the super cell $K_2(C_{22}H_{14})_2$, *a* phase (top) and *b* phase (bottom). The triclinic lattice vectors **a**, **b**, and **c** are shown.

We stress that the structure shown at the top in Fig. 1 is the ground state from both MD and DFT calculations. The lattice constants are, in fact, very similar in both types of calculations. For comparison, in Fig. 1 is also shown the metastable structure which is obtained by intercalating one more potassium ion into the ground state $K_1(C_{22}H_{14})_2$ system and let this system relax to the local energy minimum. This phase is referred to as the *b* phase in the discussion below. The difference in total energy between the *a* phase of $K_2(C_{22}H_{14})_2$ and the metastable layered *b* phase, as obtained from the DFT calculations, is 0.86 eV per super cell.

The change in position of the potassium ions from the interlayer positions in $K_1(C_{22}H_{14})_2$ to the intermolecular position in $K_2(C_{22}H_{14})_2$ is driven by the electrostatic interactions. The electrostatic energy of the system is minimized when the potassium ions are as close as possible to the center of the charged PEN molecules. In the lightly doped case this energy is still not enough to change the structure, but in $K_2(C_{22}H_{14})_2$ this effect dominates over the energy terms which keep the molecules together.

The *a* phase has a completely different anisotropic behavior as compared to the *b* phase, which affects the electronic properties quite dramatically. Figures 2 and 3 show the electronic band structure for the two $K_2(C_{22}H_{14})_2$ phases shown in Fig. 1. The four pairs of bands shown are the bonding and antibonding linear combinations of the PEN dimer wave functions corresponding to the two highest occupied (HOMO and HOMO-1) and the two lowest unoccupied (LUMO and LUMO+1) PEN molecular orbitals.

The *k*-space directions shown in Figs. 2 and 3 have been chosen in order to display directions with high energy dis-

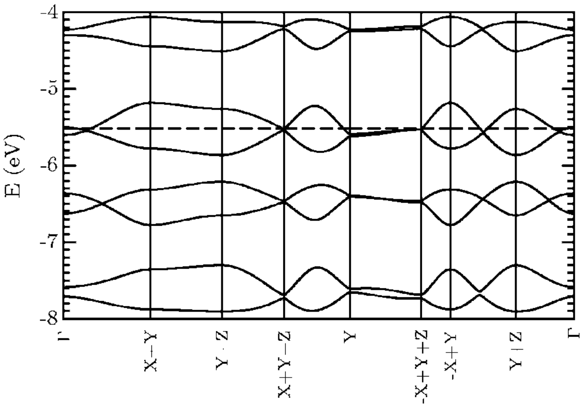

FIG. 2. Band structure of the the super cell $K_2(C_{22}H_{14})_2$ (*a* phase) from the Γ point and between linear combinations of the BZ boundary points *X*, *Y*, and *Z*. The coordinates of these BZ points are 000, $\frac{1}{2}00$, $0\frac{1}{2}0$, $00\frac{1}{2}$ (in the basis of the reciprocal lattice vectors $\mathbf{a}^*$, $\mathbf{b}^*$, and $\mathbf{c}^*$). The horizontal dashed line shows the Fermi level.

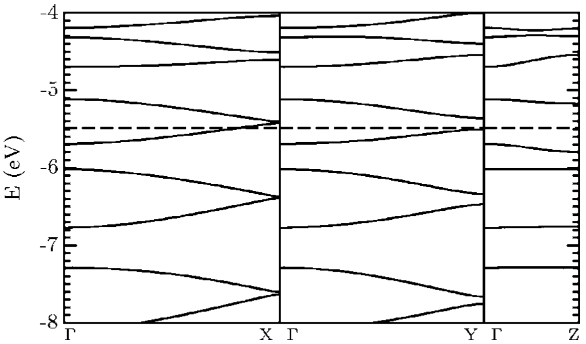

FIG. 3. Band structure of the $K_2(C_{22}H_{14})_2$ (*b* phase) between the Γ point and *X*, *Y*, and *Z*. The horizontal dashed line shows the Fermi level.

persion. In the case of the *a* phase, except for the Γ point, the directions chosen all lie on the surface of the BZ, in the $\mathbf{a}^*\mathbf{c}^*$ plane at $(0\frac{1}{2}0)$. The band structure of the metastable *b* phase is included for comparison. In this case the electronic bands are shown in the directions from the Γ point, along the reciprocal lattice vectors $\mathbf{a}^*$, $\mathbf{b}^*$, and $\mathbf{c}^*$, respectively.

The band dispersion can be discussed in terms of the strength of the splitting between the bonding and antibonding orbitals of the PEN dimer super cell. We note immediately from Fig. 2 that this splitting is qualitatively the same for all bands, i.e., the internal structure of the HOMO and LUMO orbitals do not affect the electronic properties to a large extent. Instead, the strength of the splitting is determined by the wave vector of the propagating wave functions. In the directions given by the BZ surface points *Y*, $X+Y+Z$, and $-X+Y+Z$, the bonding and antibonding states are degenerate (HOMO and LUMO bands) or nearly degenerate (HOMO-1 and LUMO+1 bands). Large splittings are obtained for the set of BZ points $X+Y$, $Y+Z$, $-X+Y$, and $Y-Z$ and also along a straight line connecting the points $X+Y+Z$ and *Y*. We also note that large splittings are maintained when the reciprocal lattice vectors are changed from $X+Y$ to $Y+Z$, whereas near degeneracies (avoided crossings) there occur for bonding and antibonding levels between *Y* and $-X+Y+Z$.

The *a*-phase lattice vectors **a**, **b**, and **c** are close to orthogonal which results in reciprocal lattice vectors $\mathbf{a}^*$, $\mathbf{b}^*$, and $\mathbf{c}^*$ that are approximately parallel to **a**, **b**, and **c**, respectively. It is, therefore, straight forward to interpret points in the reciprocal space with strong (weak) splittings as real space directions of large (small) effective overlaps of the molecular wave functions. We note that the *a* phase shows dispersion as a function of changes in the $\mathbf{c}^*$ coordinate, which is not the case neither for the *b* phase (shown in Fig. 2) nor for pristine PEN.[9,10] This is a direct consequence of the sliding of the neighboring PEN molecules which increases the π-π overlap in the **c** direction and also results in a strong reduction in the overlap along the **a** and **b** directions as compared to the *b* phase.

The differences in anisotropy of the band structure compared to the pristine phase should also appear in the charge carrier mobility. The π-π overlap in the **c** direction of the *a* phase also allows for high mobility in directions which has a component in the **c** direction, in sharp contrast to the layered phase of the pristine system which has a much higher mobility within the **ab** plane than along the **c** direction.

The bandwidth of the half-filled conduction band in the *a* phase is 0.7 eV, which is larger than in pristine PEN for which we obtain 0.5 eV for the LUMO band and 0.3 eV for the HOMO band. Also the *b* phase results in a width of the conduction band of 0.7 eV. In both the *a* and *b* phases of $K_2(C_{22}H_{14})_2$ the structure closely resembles a π-stack arrangement. This arrangement clearly has an advantage in terms of intermolecular π-π overlap as compared to the herringbone structure of the pristine system, which explains the higher bandwidths in the doped phases.

The Fermi energy of the $K_2(C_{22}H_{14})_2$ system lies approximately between the two bands corresponding to the LUMO's of the neutral dimer indicating a near complete charge transfer from the two K atoms in the super cell to the PEN molecules. Thus, the perfectly ordered system is metallic which explains the increase in conductivity observed experimentally in potassium-doped PEN.[12] In addition, the large amount of charge carriers present in the doped system and the possibility of forming quite extended states in some directions certainly indicate a highly conducting state even for moderately disordered systems.

Figure 4 shows the density of states for the *a* and *b* phases

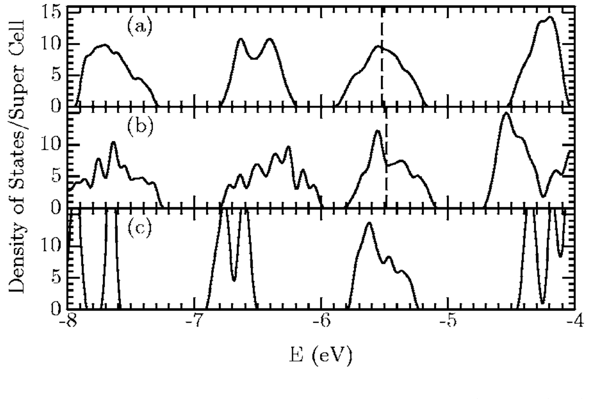

FIG. 4. Density of states for the super cell $K_2(C_{22}H_{14})_2$ (a) *a* phase, and (b) *b* phase, and (c) pristine PEN. The vertical dashed line shows the Fermi level.

of $K_2(C_{22}H_{14})_2$ and for the pristine $(C_{22}H_{14})_2$ system. The overall structure for the *a* and *b* phases is the same; the Fermi energy appears in the middle of the LUMO band of the pristine system and the bands are located in the same energy regime in both cases. As discussed above, the bandwidths are larger for the doped systems than for pristine PEN. The most notable difference between the *a* and *b* phase is observed in the internal structure of the bands. The *b* phase HOMO bandwidth is 0.8 eV, which is considerably larger than in the *a* phase, and shows an oscillating structure.

IV. SUMMARY AND CONCLUSIONS

In conclusion, from MD and DFT calculations we have identified a structural phase transition in potassium-doped PEN. The phase transition occurs when two potassium ions are occupying each super cell. The structural changes are rationalized in terms of a sliding of adjacent PEN molecules relative to each other, which allows for the potassium ions to come close to the center of the PEN molecules. This change in structure occurs as a result of electrostatic interactions between dopant and the PEN molecules. The new stable phase with two potassium ions per super cell has an electronic structure with dispersive bands along the pitch directions, which is completely different from the electronic structure of the layered pristine phase.

ACKNOWLEDGMENTS

Financial support from the Swedish Research Council (VR) is gratefully acknowledged. We also thank the Swedish National Infrastructure Committee (SNIC) for providing computational facilities.

---

*Electronic address: andha@ifm.liu.se
†Electronic address: joboh@ifm.liu.se
‡Electronic address: sst@ifm.liu.se

[1] N. Karl, *Organic Semiconductors*, Landolt Börnstein, New Series, Group III, Vol. 17 (Springer, Berlin, 1985).
[2] C. D. Dimitrakopoulos and P. R. L. Malenfant, Adv. Mater. (Weinheim, Ger.) **14**, 99 (2002).
[3] P. Batail, Chem. Rev. (Washington, D.C.) **104**, 4887 (2004).
[4] S. F. Nelson, Y.-Y. Lin, D. J. Gundlach, and T. N. Jackson, Appl. Phys. Lett. **72**, 1854 (1998).
[5] G. A. de Wijs, C. C. Mattheus, R. A. de Groot, and T. T. M. Palstra, Synth. Met. **139**, 109 (2003).
[6] O. D. Jurchescu, T. Baas, and T. T. M. Palstra, Appl. Phys. Lett. **84**, 3061 (2004).
[7] Y.-Y. Lin, D. J. Gundlach, S. F. Nelson, and T. N. Jackson, IEEE Trans. Electron Devices **44**, 1325 (1997).
[8] C. C. Mattheus, A. B. Dros, J. Baas, G. T. Oostergetel, A. Meetsma, J. L. de Boer, and T. T. M. Palstra, Synth. Met. **138**, 475 (2003).
[9] J. Cornil, J. P. Calbert, and J. L. Brédas, J. Am. Chem. Soc. **123**, 1250 (2004).
[10] R. G. Endres, C. Y. Fong, L. H. Yang, G. Witte, and C. Wöll, Comput. Mater. Sci. **29**, 362 (2004).
[11] T. Minakata, I. Nagoya, and M. Ozaki, J. Appl. Phys. **69**, 7354 (1991).
[12] T. Minakata, M. Ozaki, and H. Imai, J. Appl. Phys. **74**, 1079 (1993).
[13] M. Cazayous, A. Sacuto, G. Horowitz, P. Lang, A. Zimmers, and R. P. S. M. Lobo, Phys. Rev. B **70**, 081309(R) (2004).
[14] B. Fang, H. Zhou, and I. Honma, Appl. Phys. Lett. **86**, 261909 (2005).
[15] W. Gao and A. Kahn, J. Appl. Phys. **94**, 359 (2003).
[16] T. Ito, T. Mitani, T. Takenobu, and Y. Iwasa, J. Phys. Chem. Solids **65**, 609 (2004).
[17] T. Mori and S. Ikehata, J. Appl. Phys. **82**, 5670 (1997).
[18] G. Gao, T. Çağin, and William A. Goddard III, Phys. Rev. Lett. **80**, 5556 (1998).
[19] R. B. Brooks, R. E. Bruccoleri, B. D. Olafson, D. J. State, S. Swaminathan, and M. Karplus, J. Comput. Chem. **4**, 187 (1983).
[20] L. Nilsson and M. Karplus, J. Comput. Chem. **7**, 591 (1986).
[21] A. D. MacKerell, Jr., D. Bashford, R. L. Bellott, R. L. Dunbrack, Jr., J. D. Evanseck, M. J. Field, S. Fischer, J. Gao, H. Guo, and S. Ha, J. Phys. Chem. **102**, 3586 (1998).
[22] G. Kresse and J. Hafner, Phys. Rev. B **47**, R558 (1993).
[23] G. Kresse and J. Furthmüller, Comput. Mater. Sci. **6**, 15 (1996).
[24] G. Kresse and J. Furthmüller, Phys. Rev. B **54**, 11169 (1996).
[25] Y. Wang and J. P. Perdew, Phys. Rev. B **44**, 13298 (1991).
[26] J. P. Perdew, *Electronic Structure of Solids '91* (Akademie Verlag, Berlin, 1991).